

Demonstration and design of a compact diffraction limited spectrograph.

Christopher H. Betters^{*a,b}, Sergio G. Leon-Saval^a, Joss Bland-Hawthorn^{a,b}, Gordon Robertson^b.

^aInstitute of Photonics and Optical Science, School of Physics, University of Sydney, Australia

^bSydney Institute for Astronomy, School of Physics, University of Sydney, Australia

ABSTRACT

PIMMS IR is a prototype high resolution diffraction limited spectrograph operating in the near infrared. Its current configuration has a bandwidth of 8nm centred on 1550nm with a resolving power, $\lambda/\Delta\lambda$, of 31000 with the option to increase this to ~60000 using a dual grating system. Remarkably, this is 85% of the theoretical limit for Gaussian illumination of a diffraction grating. It is based upon the PIMMS#0 (photonic integrated multi-mode micro-spectrograph), a design that utilises the multi-mode to single-mode conversion of the photonic lantern. By feeding the spectrograph with the single-mode fibres we are able to design and build a spectrograph whose performance is diffraction limited and independent of the input source (i.e. a telescope) it is attached to. The spectrograph has with a throughput of ~70% (that is the light from the single-mode entrance slit that lands on the detector). The spectrograph is also extremely compact with a footprint of just 450mm x 190mm. Here we present the design of PIMMS IR and its performance characteristics determined from ray tracing, physical optics simulations and experimental measurements.

Keywords: astronomical instrumentation: diffraction limited; instrumentation: spectrographs; high resolution; Gaussian beam and astrophotonics

1. INTRODUCTION

Conventional astronomical spectrographs often use multi-mode optical fibres (MMFs) to feed light from a telescope to the spectrograph slit. This has been an extremely successful technique, enabling flexible observations of 100s to 1000s of objects at once. However, these spectrographs are inherently limited in their performance (spectral resolution and throughput) by the size of the entrance slit (either the MMF itself or a slit that masks the MMF, thus losing light). A diffraction limited slit (i.e. the smallest possible), while allowing for diffraction limited spectral resolution, would have extremely poor throughput if combined with a conventional MMF.

Efficient diffraction limited spectroscopy, on the other hand, is possible via single-mode fibres (SMFs). The light in a SMF is guided as a fundamental Gaussian beam — analogous to the diffraction limited focus of telescope — forming the smallest possible input slit for a spectrograph. The simple nature of the SMF output also exhibits very little scattering compared to MMF inputs, resulting in cleaner PSFs. Previously, SMFs were not feasibly for astronomical applications due to the difficulty of coupling light into the fibres efficiently. However, the use of SMFs is now a viable option thanks to the efficient multi-mode (MM) to single-mode (SM) converter known as the photonic lantern.¹⁻³

The conversion from MM to SM also decouples the spectrograph design from the light source at the MM input. The spectrograph design no longer need match the focal ratio of a telescope beam, rather it is designed to match the output of an array of SMFs (which remain unchanged regardless of what the source at the MM input is). The conversion to SM also allows various advances that harness technologies limited to SMFs to be incorporated into new and pre-existing spectrographs. These include:

- Broadband spectral suppression: 103 of brightest hydroxyl emission lines between 1.47 and 1.70 μm were suppressed using a photonic lantern and fibre Bragg grating feed to the IRIS2 instrument on the AAT.^{4,5}

^{*}c.bettters@physics.usyd.edu.au

- Integrated Photonic Spectrograph (IPS): An arrayed waveguide grating based spectrograph was demonstrated at the AAT operating in the astronomical H-band atmospheric window (1485–1825 nm). Using phased waveguides to mimic a diffraction grating, this ‘spectrograph on a chip’, achieved a resolving power of $R = 7000$.^{6,7}
- and Here we present the first implementation of a high resolution PIMMS#0⁸ type spectrograph dubbed PIMMS IR. As a photonic lantern allows for a spectrograph to be fed by an array of SMFs, the design achieves true diffraction limited performance in a compact package. It can also incorporate targeted spectral suppression or compact laser frequency combs for precision spectroscopy.⁹

In this paper we describe the design considerations that must be taken into account for a diffraction limited spectrograph fed by SMFs. This is followed by the optical design and performance of PIMMS IR, and finally we present the initial testing of the spectrograph.

2. SPECTROGRAPH DESIGN AT THE DIFFRACTION LIMIT

The optical design of PIMMS IR must be diffraction limited in order to take full advantage of the SMF input. As the output of a SMF is a fundamental Gaussian beam (with a waist ω_0) the PIMMS IR optics must collimate and refocus the beam without significant aberration (i.e. produce a Gaussian PSF with a waist $M\omega_0$, where M is the magnification of the system) in order to attain a diffraction limited spectral resolution. Conveniently, Gaussian beams are particularly resistant to aberrations as most of their power is located at the centre of the beam. The key challenge in dealing with a Gaussian beam is that there is no well defined edge, thus it will be truncated to some extent by the optics. Even slight truncation can lead to a broadening of the PSF at the focus, despite minimal loss of power. The literature suggests that an aperture, with diameter D_{apt} , should be greater than three times the $1/e^2$ width, $2\omega_0$, of an incident beam in order for diffraction effects to be negligible.^{10,11} However, this does not take into account that the Gaussian beam would appear elliptical if the circular aperture is at an angle with respect to the direction of the beam, as is the case for a diffraction grating. For small angles of incidence this effect would presumably be small, but at high angles of incidence (such as those required by high line density gratings), we need to consider the implications. Here we use the physical optics facility of ZEMAX^a to determine the optimal ratio of the aperture width and beam width where the angle of incidence on the diffraction grating is $\theta_i = 60$ degrees.

To investigate the effects of the diffraction grating aperture we begin the simulation with a Gaussian beam with a waist, $\omega_0 = 5.25\mu\text{m}$ (consistent with the output of a SMF-28 fibre). This is collimated with a ‘perfect lens’ to form a beam with a waist ω_r . In a Littrow configuration the beam is projected on to the diffraction grating as $1/\cos\theta_i$ in the dispersion axis, while remaining the same width in the cross-dispersion axis. The radius, r , of the diffraction grating is varied from 0.8 to 3 times $\omega_r/\cos\theta_i$. This is then then focused using another ‘perfect lens’ and the beam waist of the image, ω_f , measured using a Gaussian fit and normalised by ω_0 . ZEMAX also provides a beam quality factor or M^2 value.^{12,13} As the M^2 value approaches unity, the closer to a perfect Gaussian the beam actually is. This can be seen in Fig. 1, when the aperture, with radius r , is similar in size to ω_0 , the beam is broadened at focus and the M^2 value quickly departs from unity. As the aperture size increases, diffraction effects become negligible and the beam approaches an unperturbed Gaussian with a normalised width of unity. For gratings with $r > 4\omega_r$ — or r is greater than twice the width beam projected on the grating — it is apparent that broadening effects are minimal.

We must also consider the spectral resolving power ($R = \lambda/\Delta\lambda$) for the case of Gaussian illumination of the diffraction grating. We determine this by equating the size of resolution element in the focal plane and the displacement due to $\Delta\lambda$ given by the standard grating equation ($\sin\theta_i + \sin\theta = m\lambda/d$) with the Littrow condition ($\theta_i = \theta$; incident angle = diffracted angle). This is described in detail by Robertson et al.,¹⁴ but briefly it is as follows:

^a<http://www.radiantzemax.com>

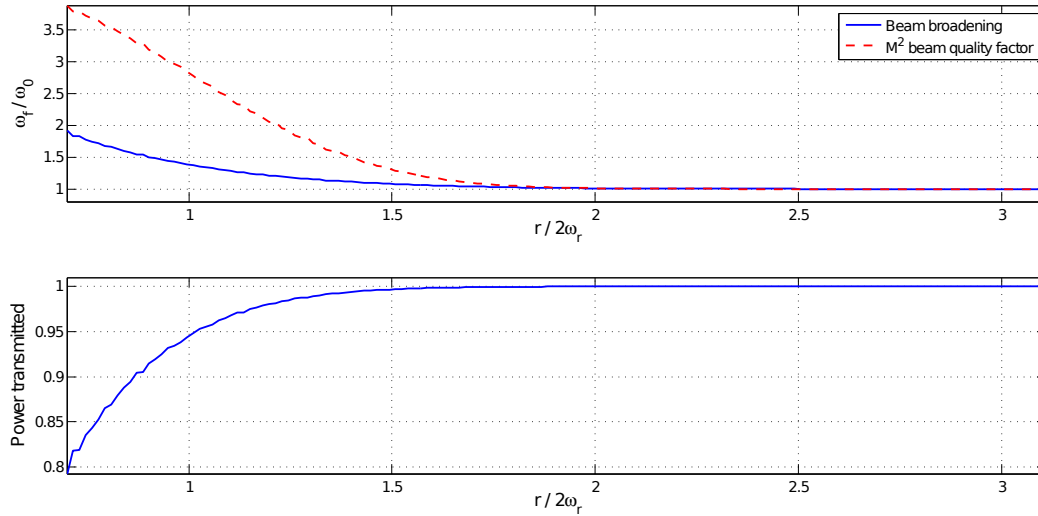


Figure 1: Top: The solid blue line is the PSF width, ω_f , normalised by the expected width, ω_0 , for each aperture to beam radius ratio (i.e. ω_f/ω_0). The M^2 beam quality factor (red dashed line) is given to illustrate the effect even a small amount of truncation has on a Gaussian beam. For even very small power losses it departs from unity. Bottom: The total transmitted power is given where the initial power was 1.

The resolution element is given by the 1.119 times the FWHM of the PSF at the detector (the 1.119 factor provides the same contrast for neighbouring Gaussians as the Rayleigh criterion does for Airy patterns),

$$\text{PSF}_{\text{FWHM}} = 1.119 \times f_{\text{cam}} \frac{\lambda}{d_{1/e^2}} \frac{2\sqrt{\log 4}}{\pi}, \quad (1)$$

where f_{cam} is the focal length of the camera and d_{1/e^2} ^b is the beam diameter. The $\Delta\lambda$ displacement is given by,

$$\text{disp}_{\Delta\lambda} = 2f_{\text{cam}} \tan \theta_i \frac{\Delta\lambda}{\lambda_c}. \quad (2)$$

When Eqn. 1 and Eqn. 2 are combined we get the following expression for the resolution limit of a Gaussian illuminated grating,

$$R = \frac{\lambda}{\Delta\lambda} = 2.38 \frac{d_{1/e^2} \tan \theta_i}{\lambda}. \quad (3)$$

It is important to note that Eqn. 3 assumes no truncation of the Gaussian has occurred (i.e. $D_{\text{apt}} \gg d_{1/e^2}$). These parameters are used as a starting point in the optical design and used to refine the design in order to maximise the performance achieved using available optics.

3. OPTICAL DESIGN

PIMMS IR is by design extremely modular, allowing for laboratory testing of other astrophotonics technologies. By substituting different diffraction gratings we can quickly tune the wavelength coverage and spectral resolution of the spectrograph to suit a specific test. Further the input slit can easily be changed to interface with other instruments. For example, the central wavelength (and thus the wavelength coverage) can be adjusted by decreasing or increasing the Littrow angle (within the wavelength range supported by the grating). Additionally there are plans to expand the current configuration with a 2nd identical grating, thus increasing the resolving power by a factor of two with minimal changes to the camera and collimator configuration (although this does reduce the wavelength coverage by half). Presented here is the single grating R~30000 mode of PIMMS IR, centred on 1550nm, where it is fed diffraction limited light (i.e. fundamental Gaussian beams) by a pseudo slit formed of an array of SMFs.

^bFWHM is related to the $1/e^2$ width as: $2\omega = d_{1/e^2} = 2/\sqrt{2 \ln 2} \times \text{FWHM}$

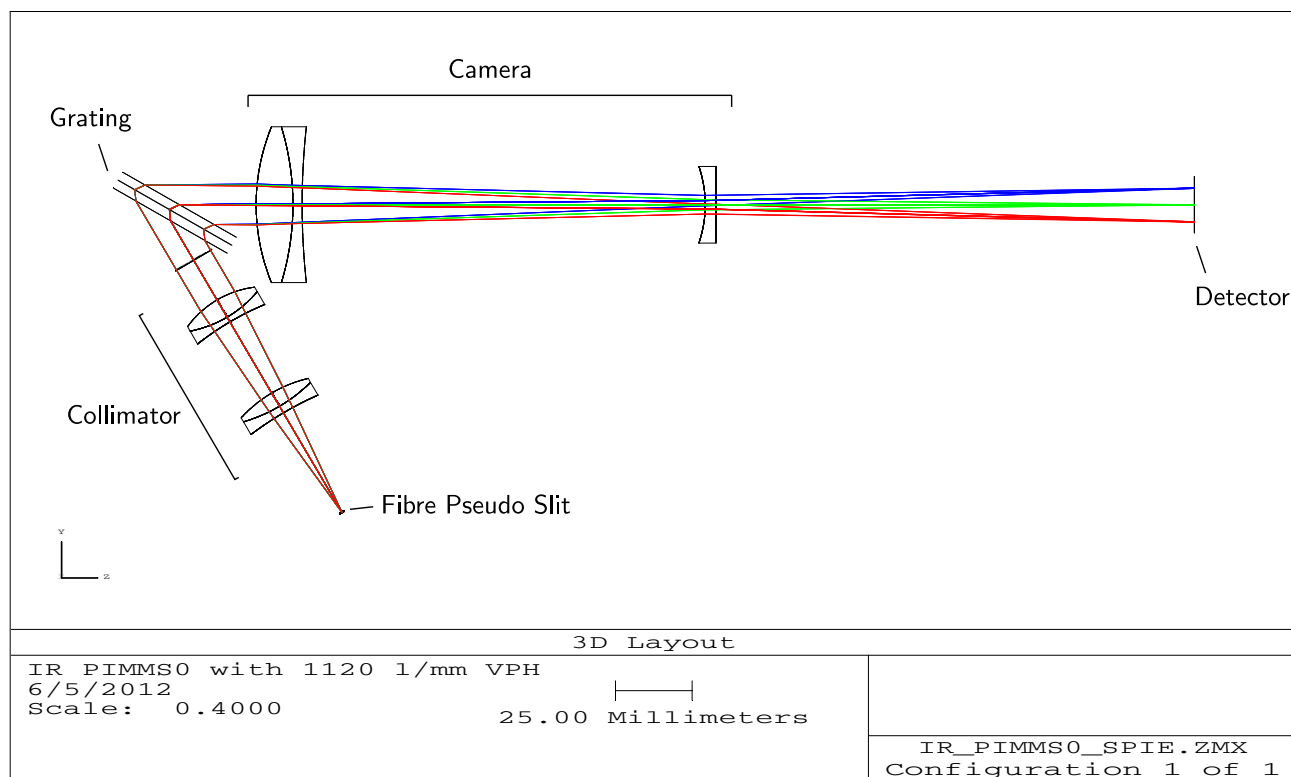


Figure 2: Optical layout of the R=31000 version of the IR PIMMS design drawn at 0.4 times actual size. The wavelengths shown are 1550 ± 4 nm. The collimator uses 1in optics, while the camera uses a combination of 2" and 1" optics. With the addition of a detector package the design fits within an area 450mm long and 190mm wide.

A typical SMF output in the near IR is an $f/5$ ($NA \approx 0.1$ or $\omega_0 = 5.25\mu m$) Gaussian beam. Given the diffraction limited nature of the SMF output, the guiding element in the overall design of the spectrograph is the size of the diffraction grating (as $R \propto$ number of grating lines illuminated). The size of the diffraction grating along with the considerations discussed in Sec. 2 for a Gaussian beam thus determine the $f/\#$ required of the collimator. The required camera $f/\#$ is then determined by the size of the detector pixels.

3.1 Grating

Our initial inclination was to use ‘off the shelf’ components for the entire instrument, however in order to maximise the spectral dispersion performance of the complete spectrograph we opted for a custom Wastach Photonics^c volume phase holographic (VPH) grating as the primary dispersing element. This grating is 2" (50.8 cm, with a 42.8mm clear aperture) in diameter with an equivalent ruling of 1120 l/mm. At the design wavelength of 1550nm it is has an overall efficiency of 80% dropping to $\sim 75\%$ at 1540nm. The Littrow grating angle at 1550nm is 60 degrees. The high angle of incidence means that the collimated beam size can (and must) be substantially smaller than the grating (as it will be projected on the grating by a factor of $1/\cos \theta_i$, or a factor of 2 in this case). This allows for a shorter focal length collimator than a lower line density grating of the same size would require to be efficiently illuminated. It also follows that a shorter focal length camera is required to attain adequate sampling in the focal plane and thus an advantageously smaller overall setup (decreased footprint, smaller optics etc.) is achieved.

3.2 Collimator

In Sec. 2 the simulations of a Gaussian beam truncation indicated that the optimal beam width should not exceed 2 times the limiting aperture in the system. Using this as a starting point we see that the ϕ 42.8mm clear

^c<http://wasatchphotonics.com/>

aperture of our VPH results in a maximum beam diameter, d_{max} , of ~ 21.4 mm. This is however the projected beam width on the grating. The beam size produced by the collimator is thus limited to $d_{max} \cos \theta_i = 2\omega_r$. Consequently the beam from the collimator should have a width of order ~ 11 mm at 1550nm for the grating selected above.

This beam width corresponds to a collimator with a focal length close to 55mm for the output of a SMF. In order to achieve a diffraction limited system, a pair of achromatic doublets are used to collimate the beam. Several pairs were tested both via spot diagrams, and if performance appeared expectable, physical optics propagation (POP). The final pair selected are both 1" achromatic doublets manufactured by Thorlabs, the first with a focal length of with a 150mm and the second 100mm. The two are separated by 26.9 mm of air (determined via a combination of the ray tracing optimisation of the separation, POP simulations of the beam quality and lengths of lens tubes required to easily mount the optics). The optimal focal length of the collimator is 68.6mm, resulting in a beam diameter of ~ 13 mm, or a $r/2\omega_r$ ratio of 1.6. With this beam width the collimator does introduce broadening in the focal PSF of $\sim 10\%$. This was estimated by comparing the camera focal lengths required to an form equal width PSF for the PIMMS IR collimator and an equivalent perfect lens. The truncation introduced was a necessary compromise as a shorter focal length configurations tested produced poorer optical performance, which would have lead to even more significant broadening.

3.3 Detector and camera

The ideal detector for PIMMS IR would have rectangular pixels that are $3\mu\text{m}$ wide and several microns tall. This would allow the most compact design, and reduce read the noise build up encountered when summing the pixel in the cross-dispersion direction. PIMMS IR, has a much simpler detector, the Xenics^d Xeva 1.7 320 InGaAs detector. It's 320x240 array of $30\mu\text{m}$ pixels is sensitive to the NIR ($1\mu\text{m}$ to $1.7\mu\text{m}$). In order to correctly sample spectra at the detector (i.e. > 2 pixel per FWHM) the magnification required from the collimator and camera is given by the ratio of the FWHM mode field diameter of a single-mode input fibre ($6.2\mu\text{m}$ for SMF-28) and the width of two pixels (i.e. $M = 60\mu\text{m}/6.2\mu\text{m} = 9.7$). So the magnification ratio provided by the collimator and camera needs to be of order 10 or a camera focal length close to ~ 680 mm. However, due to broadening effects, the desired focal length to achieve 2 pixels per FWHM sampling was only 540mm.

The focal length difference indicates that the broadening caused by the optics and diffraction grating is of order 20%. This is consistent with the beam broadening due to truncation at $r/2\omega_r = 1.6$ combined with the 10% broadening due to the collimator. The camera takes the form of simple telephoto lens constructed with a 200mm achromatic doublet and a -75mm plano-concave lens. As the focal length is 540mm and a total length of 280mm it has a telephoto ratio of ~ 0.5 . It is important to reiterate that the camera would be much smaller/shorter if the detector pixels were smaller, but that PIMMS IR is very close to the minimal configuration possible.

4. PERFORMANCE

4.1 ZEMAX Simulation

ZEMAX spot diagrams for evenly spaced fibre positions along the length of the spectrograph slit are shown in Fig. 3. The spot diagrams show relatively uniform performance on and off axis. Position 1 corresponds to an on-axis fibre and position 2 corresponds to furthest position off-axis the fibre can be placed on the slit while still forming an image on the Xenics detector. The 3rd position corresponds to a rough limit on the size of the slit before the collimator design must be revisited. The wavelength range shown has a bandwidth of 20nm centred on 1550nm. The central 8nm correspond to the bandwidth seen by the PIMMS IR detector, while the extended range is the bandwidth that could be seen by a $2k \times 15\mu\text{m}$ pixel array. A ray tracing estimated of throughput, including anti-reflective coatings on optics and diffraction grating efficiency, is approximately 70%. POP simulations predict that approximately 1% of the power loss is lost due to truncation of the beam.

The Airy disk shown in Fig. 3 is calculated by ZEMAX as '1.22 times the wavelength times the F/# of the beam'. It does not consider diffraction, but provides a reasonable estimate as to how well the system is performing. All the spot diagrams indicate that the system should be diffraction limited as rays are confined

^d<http://www.xenics.com/>

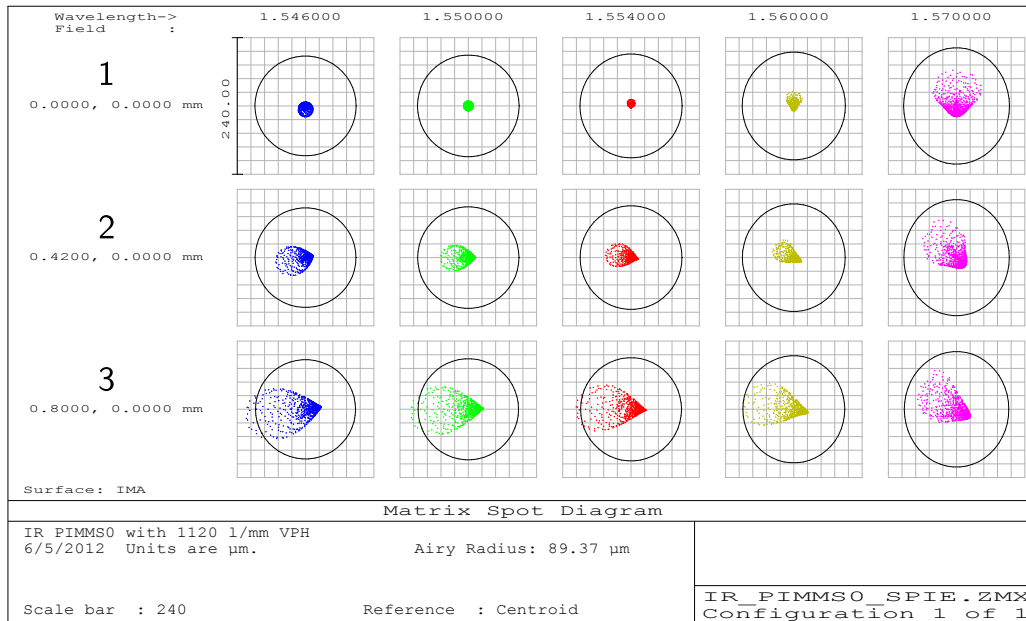


Figure 3: Spot diagrams for field position: 1 -on-axis, 2 - edge of Xenics camera FOV and 3 - Edge of diffraction limited optical performance. Wavelength coverage is: $1550 \pm 4\text{nm}$ for the PIMMS IR detector and $1550 \pm 10\text{nm}$ corresponding to a 2K detector with $0.15\mu\text{m}$ pixels.

within the Airy disk. The wavefront error of the system further supports this. The maximum peak to valley (PTV) error is 0.22 waves with an RMS of 0.036 (found at the edges of the detector), fulfilling both the Rayleigh $1/4$ wave PTV criteria and $1/14$ wave RMS wavefront error criteria for diffraction limited optics.

To confirm a Gaussian PSF, and thus the diffraction limited nature of the system, we inspect the POP simulations of the propagation. This implies that beam should have an M^2 value close to unity. Typical profiles for the on-axis input are shown in Fig. 4. Each has an M^2 value close to 1.2. It is assumed that this departure from a perfect Gaussian is predominantly due to truncation of the Gaussian at the collimator and diffraction grating as discussed previously. Using POP simulations we confirm that the nominal beam width, d_{1/e^2} , incident on the grating is 13.00 mm. Using this we see that the maximum resolving power of the spectrograph could attain according to Eqn. 3 is ~ 35000 at 1550nm.

We measure resolution in ZEMAX using the width of the POP profile, assigning a wavelength scale using the linear dispersion determined via ray tracing. The same resolution element specified in Eqn. 1 is used in calculating the resolving power ($1.119 \times \text{FWHM}$). A summary of the resolving powers measured in this way at the primary wavelengths and field positions can be seen in Table. 1. Remarkably, these values are about 85% the theoretical maximum values, indicating we have indeed achieved a reasonable balance between grating illumination and truncation.

Table 1: Resolving power ($\lambda/\Delta\lambda$) over the specified wavelength range at the edges and centre of the detector. Measured for POP simulations.

Wavelength (nm)	Position off Axis μm		Theoretical
	0	420	
1546	31300	30600	34500
1550	30900	30600	35000
1554	30200	30200	35500

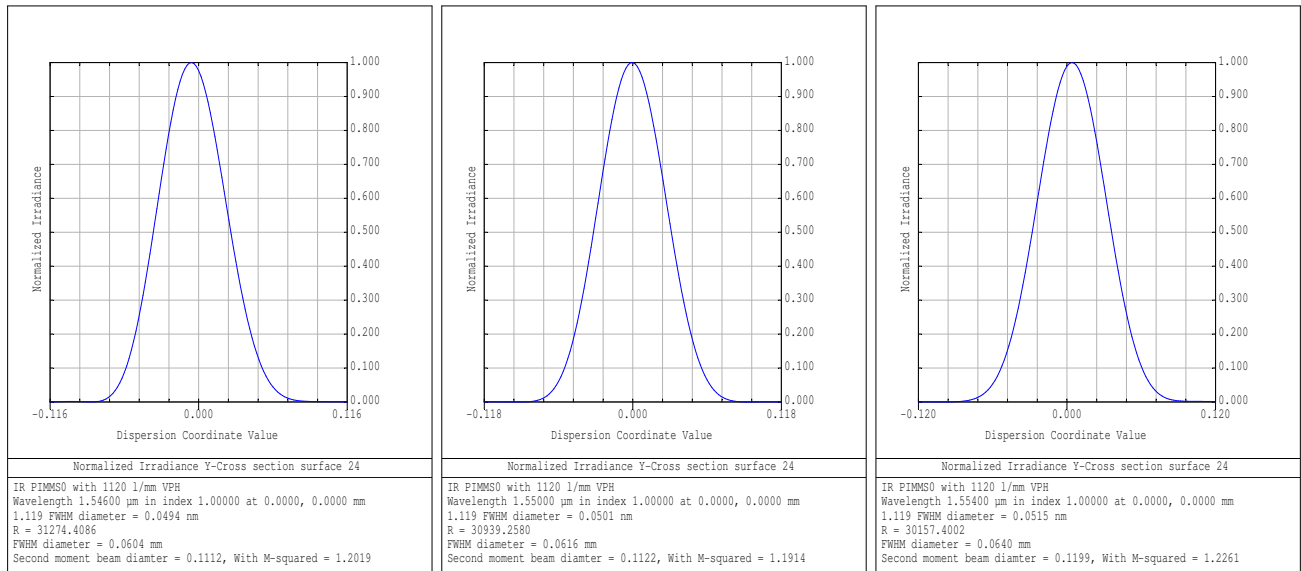


Figure 4: Physical optics profiles in the spectral direction for a fibre on-axis. Included is the spectral resolution element in nm, the FWHM determined from the plot and the ISO standard 11146 second moment width and beam quality factor.^{12, 15}

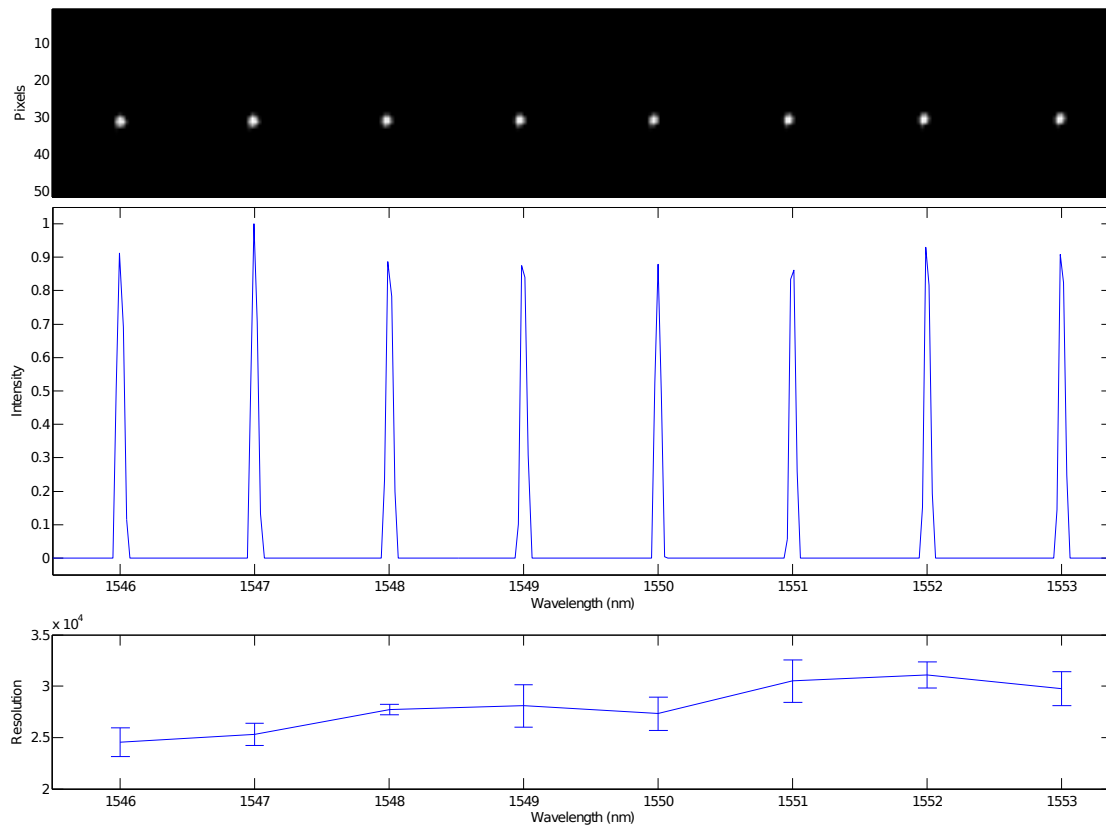


Figure 5: Top: Cropped raw spectrum from PIMMS IR initial testing. Image is 50x320 pixels. Each spot is separated by 1nm. Middle: 1D extracted spectrum, wavelength calibrated using the laser lines. Bottom: Resolution of each laser line calculated as $\lambda/(1.119 \times \text{FWHM})$ with 95% confidence interval of Gaussian width fit as the error.

4.2 Preliminary experimental results

PIMMS IR is not just a concept instrument, a prototype version has been constructed as described above and in initial testing performs close to specification. A sample spectrum of several laser lines (from a tuneable laser source) is shown in Fig. 5. From this, a 1D spectrum was extracted, shown in the middle of Fig. 5, using a simple tramline summation (column summation is weighted evenly). A Gaussian was fit to each line to determine an accurate position (for wavelength calibration) and the width. The bottom plot in Fig. 5 shows the resolving power of each line, where $\Delta\lambda = 1.119 \times \text{FWHM}$. The error shown is the 95% confidence interval for the width given by the Gaussian fit. Above 1550nm the resolving power is consistent with the predicted values. Below 1550 nm it is lower the predicted, but not drastically so. We thus believe further fine tuning of the setup will eliminate this discrepancy.

5. CONCLUSIONS

Here we have presented the design and demonstrated a prototype PIMMS IR diffraction limited spectrograph. Both ZEMAX ray tracing and POP show the design is indeed diffraction limited. Indeed its primary limitation appears to be diffraction of a Gaussian beam when it is truncated by an aperture. It has nonetheless been demonstrated to have a spectral resolution very close to the theoretical limit of a Gaussian illuminated diffraction grating, both in simulation and initial experimental results. Additionally it is extremely compact fitting in a space just 450mm x 190mm. With these promising initial results, it is clear that the PIMMS IR design will allow quick and effective laboratory based testing of various astrophotonic technologies and is an important pathfinder for other PIMMS based diffraction limited instruments.

REFERENCES

- [1] Leon-Saval, S. G., Birks, T. A., Bland-Hawthorn, J., and Englund, M., "Multimode fiber devices with single-mode performance," *Optics Letters* **30**, 2545–2547 (Oct. 2005).
- [2] Noordegraaf, D., Skovgaard, P. M., Nielsen, M. D., and Bland-Hawthorn, J., "Efficient multi-mode to single-mode coupling in a photonic lantern," *Optics Express* **17**, 1988–1994 (Feb. 2009).
- [3] Leon-Saval, S. G., Argyros, A., and Bland-Hawthorn, J., "Photonic lanterns: a study of light propagation in multimode to single-mode converters," *Optics Express* **18**, 8430–8439 (Apr. 2010).
- [4] Bland-Hawthorn, J., Ellis, S. C., Leon-Saval, S. G., Haynes, R., Roth, M. M., Löhmansröben, H. G., Horton, A. J., Cuby, J. G., Birks, T. A., Lawrence, J. S., Gillingham, P., Ryder, S. D., and Trinh, C., "A complex multi-notch astronomical filter to suppress the bright infrared sky," *Nature Communications* **2**, 581 (2011).
- [5] Ellis, S. C., Bland-Hawthorn, J., Lawrence, J. S., Bryant, J., Haynes, R., Horton, A., Lee, S., Leon-Saval, S., Löhmansröben, H.-G., Mladenoff, J., O'Byrne, J., Rambold, W., Roth, M., and Trinh, C., "GNOSIS: an OH suppression unit for near-infrared spectrographs," in [*Ground-based and Airborne Instrumentation for Astronomy III*], McLean, I. S., Ramsay, S. K., and Takami, H., eds., *Proc. SPIE* **7735**, 773516 (2010).
- [6] Cvetojevic, N., Lawrence, J. S., Ellis, S. C., Bland-Hawthorn, J., Haynes, R., and Horton, A., "Characterization and on-sky demonstration of an integrated photonic spectrograph for astronomy," *Optics Express* **17**, 18643–18650 (Oct 2009).
- [7] Cvetojevic, N., Jovanovic, N., Lawrence, J., Withford, M., and Bland-Hawthorn, J., "Developing arrayed waveguide grating spectrographs for multi-object astronomical spectroscopy," *Optics Express* **20**, 2062–2072 (Jan 2012).
- [8] Bland-Hawthorn, J., Lawrence, J., Robertson, G., Campbell, S., Pope, B., Betters, C., Leon-Saval, S., Birks, T., Haynes, R., Cvetojevic, N., and Jovanovic, N., "PIMMS: photonic integrated multimode microspectrograph," in [*Ground-based and Airborne Instrumentation for Astronomy III*], McLean, I. S., Ramsay, S. K., and Takami, H., eds., *Proc. SPIE* **7735**, 77350N (2010).
- [9] Lee, C., Chu, S. T., Little, B. E., Bland-Hawthorn, J., and Leon-Saval, S. G., "Portable frequency combs for optical frequency metrology," (Accepted for publication in *Optics Express*).
- [10] Belland, P. and Crenn, J. P., "Changes in the characteristics of a gaussian beam weakly diffracted by a circular aperture," *Appl. Opt.* **21**, 522–527 (Feb 1982).

- [11] Mahajan, V., [*Optical Imaging and Aberrations: Wave diffraction optics*], SPIE Optical Engineering Press, 337-366 (2001).
- [12] Siegman, A., [*Lasers*], University Science Books, 663-679 (1986).
- [13] Radiant Zemax LLC, www.zemax.com, [*Zemax 12 User's Manual*] (May 10 2012).
- [14] Robertson, G. and Bland-Hawthorn, J., "Compact high-resolution spectrographs for large and extremely large telescopes: using the diffraction limit," in [*Ground-based and Airborne Instrumentation for Astronomy IV*], *Proc. SPIE* **8446**, 844674 (2012).
- [15] ISO Standard 11146, [*Lasers and laser-related equipment – Test methods for laser beam widths, divergence angles and beam propagation ratios*] (2005).